International Journal of Applied Engineering Research ISSN 0973-4562 Volume 13, Number 1 (2018) pp. 123-130

Experimental Analysis of a Square Duct Solar Air Heater with Radiation Reflectors

Raktimjyoti Parashar[1], Saksham Pandey[1], Vishesh Hasija[1] and K. Vasudeva Karanth[1*]

[1] Department of Mechanical & Mfg. Engineering, Manipal Institute of Technology, Manipal Academy of Higher Education, Manipal 576104, Karnataka, India.

[*]Corresponding author

Orcid Id: 0000-0001-6138-1204

Abstract

Energy demand in industries is growing day by day and the largest consumption of energy is in space heating and process applications. Solar technology, especially air heaters, contribute a lot in meeting these energy demands and are widely being used for various applications. Any improvement in the performance of such collectors will contribute a lot in terms of energy that is conserved. Solar air heaters are generally rectangular in cross section and the upper surface of the duct is exposed to solar radiation. In this study a square duct with the upper and side surfaces of the square duct are made effective by introducing reflectors reflecting radiation heat on to the side walls of the absorber duct so as to improve the thermal performance and to make the collector compact in size. The mirrors which reflect solar radiation are suitably positioned so as to maximize the absorption of the solar radiation heat by the absorber air. The configuration with reflectors shows a remarkable improvement in terms of thermal performance with the convective heat transfer coefficient and Nusselt Number showing a maximum of 44% improvement over the plain configuration.

Keywords: Heat transfer, Solar radiation, Radiation reflectors, Solar air heater.

INTRODUCTION

Solar air heaters are widely used in space heating applications and for process heating in industries. It has contributed a great deal in meeting the energy demand as space heating and process heating consumes large amount of energy. It is the most economical device out of all the solar collectors. It is expected that improvement in the performance of such collectors will help conserve energy to a greater extent.

The effect of geometry on thermal performance of rectangular duct solar air heaters by using V-shaped ribs on the inside of absorber plate and its effect on fluid flow characteristics was analyzed by Abdul-Malik et al. [1]

Brij Bhushan and Ranjit [2] showed that the solar air heater thermal efficiency is low due to lower thermal conductivity of air, even though they are simple in construction for usage.

Bhagoria et al. [3] studied the effect of ribs with wedge shape for the purpose of enhancement of heat transfer capability of solar air heaters. Experimentally they showed that a remarkable enhancement of thermal performance occurred at 10^o wedge angle whereas on either surfaces of the wedge the Nusselt number decreased. The increase in wedge angle led to increase in friction factor.

Hans et al. [4] reported that the inclination and orientations of ribs with the flow direction also affects the heat transfer and friction through the roughened duct. The use of multiple V-shaped ribs results in the formation of secondary flow and hence causes more turbulence; leading to high heat transfer.

Kumar et al. [5] observed that the main reason for poor thermal conductivity of air is due to the formation of laminar sub-layer near the heat transferring surface and hence for the enhancement of the heat transfer; efforts have been made to destroy the laminar sub-layer by providing artificial roughness on the heat transferring surface.

Layek et al. [6] in their experimental study of heat transfer capability and friction factor with transverse rib grooves provided on the inside of absorber plate showed remarkable enhancement in thermal performance of solar air heater.

Mohamad et al. [7] discovered a new design for the solar air heater designated as a counter flow, allowing air to pass between two glass covers. Then, the passing air reversed its direction to enter the bottom bed and passed through a wire mesh layer, which served as a supplementary absorber material.

Muluwork [8] experimented on solar air heater with discrete V-shaped staggered ribs. He found that at 60^o angle of incidence, maximum improvement in thermal performance occurred.

Varun et al. [10] stated that many researchers have used the artificial roughness by providing wires, ribs, wire-mesh, dimples and using baffles in various patterns and shapes to augment the heat transfer capability, at the cost of increase in friction factor and hence the power required to pump the air.

Circular cross-section wires, were used for roughening the surface of the absorber plate of solar air heater by Verma and Prasad et al. [11]. They determined the optimal thermo-hydraulic performance of artificially roughened solar air heaters.

It is observed from the above literature that solar air heater with treatment of the absorber plate for improvement of thermal performance has been experimented extensively. However there is a need to explore the possibility of maximizing surface area of absorber duct that is exposed to

solar radiation and hence receive maximum radiation heat. It is known that the only way to maximize the exposure of absorber duct to solar radiation is by adopting a square shaped duct and making the side walls of the duct effective in receiving solar radiation with the help of side reflectors. In this study a square duct with side reflectors is compared with that of a duct without reflectors and the thermal performances are compared to quantify the enhancement in heat transfer.

EXPERIMENTAL SETUP

A. Plain Configuration

The solar air heater plain configuration consists of square aluminum duct of 92 mm side, 1 m length and 1 mm thick. The duct is mounted on a plywood base so as to insulate the bottom surface. The side walls are insulated from outside. An entrance duct and an exit duct are attached to the absorber duct to allow the flow to stabilize inside the absorber duct. The entrance and exit duct length are as per the ASHTRA standards and are of 460 mm and 230 mm length respectively. They are made up of ½ inch plywood material with proper insulation. The schematic diagram of the plain duct is as shown in figure 1.

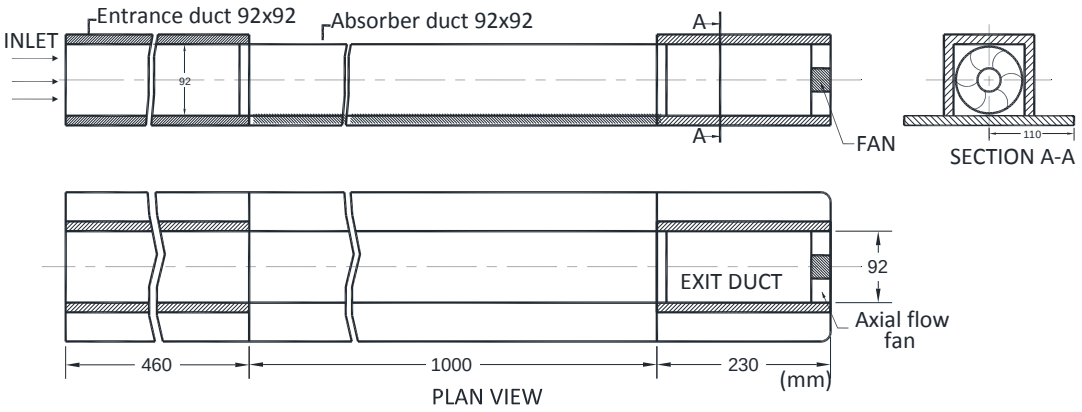

Figure 1. Sketch of the of the configuration without reflectors

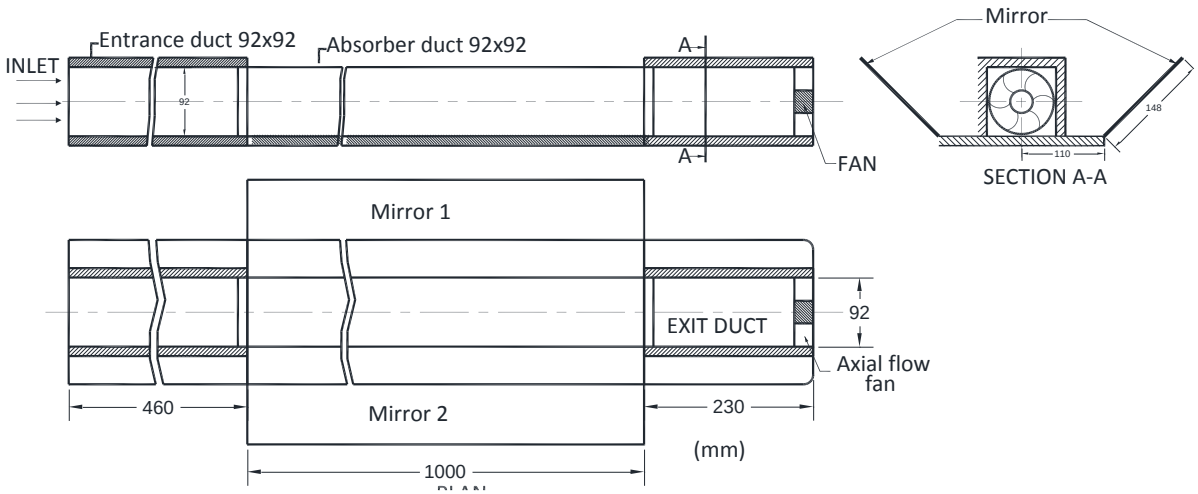

Figure 2. Schematic diagram of the air heater configuration with side reflectors

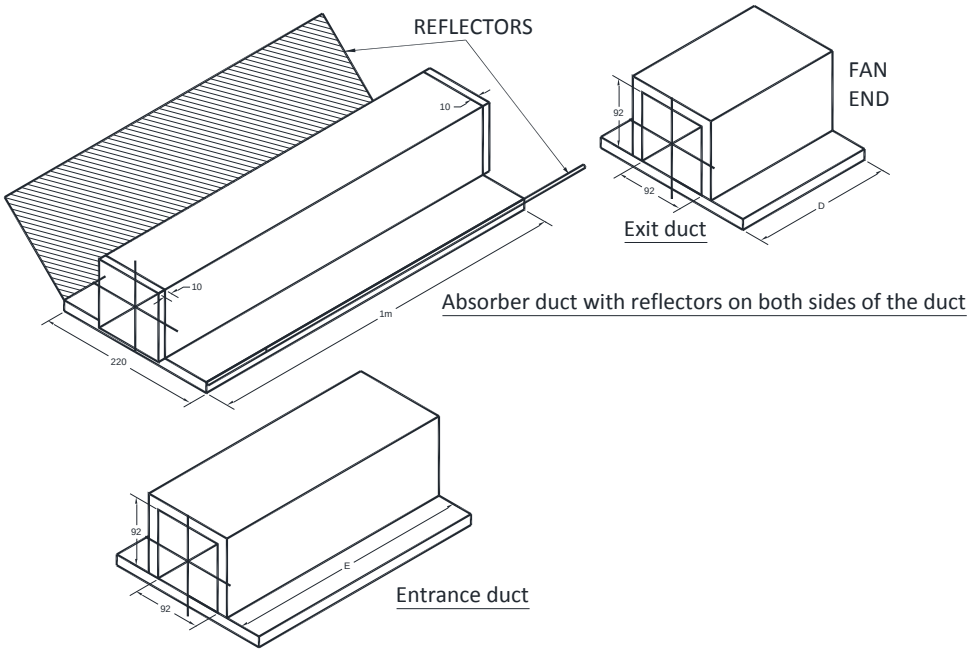

Figure 3. Isometric view of the air heater configuration with side reflectors

B. Configuration with Reflectors

The configuration with reflectors is identical to that of the plain duct except that the absorber duct is exposed to solar radiation on its side walls which are reflected from the mirrors attached to the base frame as shown in figures 2 and 3. The mirror which is hinged to the base frame can be tilted at any angle so as to completely reflect the incident radiation on to the side walls of the duct.

C. Solar fans

Two identical axial flow fans of 12 V and 0.35 amps are used to provide forced convection at varying mass flow rates inside the absorber ducts of the two configurations. The two fans are connected in parallel to a 10 W solar panel which has voltage and current characteristics as shown in figure 4.

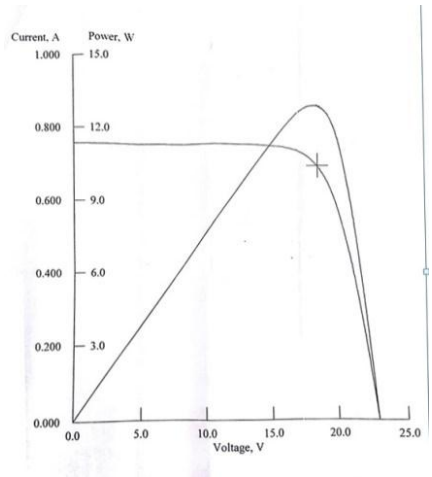

Figure 4. The voltage and current characteristics of the 10W solar panel.

A dimmer stat controller is used to vary the speed of fans at identical speeds. An electrical circuit is incorporated in the panel to provide a maximum of 12 V for the two fans as the solar panels are capable of developing a maximum of 21 V at good sunshine conditions.

EXPERIMENTATION

The experimental setup is exposed to solar radiation from 11 a.m. to 1 p.m. by tilting the air heater to 13 degree from the horizontal. The latitude of the place of experimentation is 13^o towards the north and the solar radiation will be normal to the surface when the air heater is tilted by this angle. The various performance parameters are calculated by noting the temperatures of the absorber air, absorber plate, heat flux incident on the upper surface of absorber duct and the side walls of the duct due to reflected radiation. The mass flow rate for varying speeds of the fan is also determined and is represented in terms of Reynolds number.

The temperature of the absorber air is measured using RTD type thermocouples which are mounted so that the tip of the thermocouple is at the center of the duct cross section and at locations that are critical along the flow length. The readings of thermocouple are recorded in a data logger. The absorber plate temperatures are recorded using a thermal gun by measuring the temperatures at specified marked locations on the absorber duct. The solar heat flux is recorded using a pyranometer and are recorded with respect to time as the solar flux changes with time during the period of experimentation. The mass flow rate of the air inside the duct is regulated using a dimmer stat attached to the fan and the velocity of the flow at the exit is recorded using an anemometer for various speeds of the fan. A pictorial view of the experimental setup is as shown in fig 5.

Figure 5. Image showing the two air heaters exposed to solar radiation

The plain configuration and the reflector configuration of the air heater are compared by exposing them to identical ambient conditions and the thermal performance are evaluated in terms of Nusselt number (Nu) and the convective heat transfer coefficient (h). The flow conditions are represented in terms of Reynolds number and the Nusselt number Nu. For a rectangular cross section duct, Nu is given by the Dittus-Boelter equation (1), Rosenhow and Hartnett [9].

$$Nu = 0.023\,\mathrm{Re}^{0.8}\,\mathrm{Pr}^{0.4} \quad (1)$$

The convective heat transfer coefficient 'h' is calculated using the Nusselt number. The useful heat gained by the absorber air is calculated using eq^{n}. (2),

$$Q = \dot{m}C_p\left(T_o - T_i\right) \quad (2)$$

The useful heat gain is equated to the convective heat transfer coefficient and the experimental heat transfer coefficient is determined as shown in eq^{n} (3). T_{av} is the average temperature of the air inside the absorber duct and is = $\left(T_i + T_O\right)/2$

$$h_{\exp} = \frac{Q}{A_s\left(T_s - T_{av}\right)} \quad (3)$$

The temperature of absorber air recorded by the data logger over the time period of experimentation are averaged out and adopted in the calculation of Nusselt number and heat transfer coefficient. The temperature of absorber air and the absorber duct are non-dimensionalized using equations (4) and (5) where T_i represents the ambient temperature and T_x represents the average temperature at location x along the flow path. T_s refers to the average absorber plate temperature which is recorded by the thermal gun.

$$C_T = \frac{T_x - T_i}{T_i} \quad (4)$$

$$C_{Ta} = \frac{T_s - T_i}{T_i} \quad (5)$$

The solar radiation heat flux incident on the absorber duct is recorded with the help of Pyranometer and are noted for frequent intervals during the time of experimentation for a given mass flow rate. The radiation heat flux reflected by the mirrors on the sides of the absorber duct is also noted using the pyranometer by placing it on the side walls of the absorber duct. It is observed that the reflected radiation is approximately 85 - 90% of the normal radiation heat flux.

RESULTS AND DISCUSSION

The experimentation is carried out for three days under normal sunshine conditions and the results are presented in the form of bar charts and temperature plots for the average values of the temperature. Table 1 shows the three mass flow rates at which the experiment is carried out. The characteristic length L_c is = 0.092 m as the duct is of square cross section.

Table 1: Air flow conditions adopted in the experiment

Flow velocity of air in m/s (V)	Density of air in kg/m^3 ρ	Mass flow rate in kg/s $\dot{m}$	Reynolds number $\mathrm{Re} = \frac{VL_C}{\nu}$
1.6	1.146	0.016	8674
2.9	1.146	0.028	15722
3.5	1.146	0.034	18975

Table 2 shows the thermal performance of the plain duct configuration in terms of Nusselt number and heat transfer coefficient based on Dittus-Boelter equation (1). It can be noted that the plain duct configuration has heat flux added to the absorber duct only on the top surface which is exposed to solar radiation. The Nusselt number varies from a low of 28.55 to a high of 53.4. These values are the basis of comparison for evaluating the performance of reflector configuration.

Table 3 shows the Nusselt number as determined by Dittus-Boelter equation (1) and is compared with that of Nusselt number calculated from equation (3) for the plain duct configuration. It can be noted that the two values are close to each other for the highest mass flow rates whereas for the lowest mass flow rate there exists a wide gap due to experimental errors.

Table 2: Thermal performance of the plain duct configuration based on Dittus-Boelter equation (1).

Re	Pr	Nu	h
8674	0.721	28.55	8.409
15722	0.721	45.94	13.53
18975	0.721	53.4	15.73

Table 3: Nusselt number for plain configuration

Mass flow rate in kg/s	Reynolds number Re	Nusselt number Nu from (1)	Nusselt number Nu from (3)
$m_1 = 0.016$	8674.131	28.55	37.03
$m_2 = 0.028$	15721.86	45.94	51.668
$m_3 = 0.034$	18974.66	53.4	54.227

The useful heat gain by the absorber air inside the duct is a function of the mass flow rate of the air and the temperature rise across the duct. This heat gain is also a function of surface area inside the duct and the difference between the temperatures of the absorber duct and the average temperature of absorber air. It can be noted from Table 4 that the useful heat gain is largest for the intermediate mass flow rate due to the fact that when the mass flow rate increases the temperature difference between the absorber duct and the absorber air decreases.

Table 4: Radiation heat added to absorber air for varying mass flow rates

Mass flow rate $\dot{m}$	Plain configuration		Reflector configuration	
	$(T_s - T_{av})$ ^oC	Useful heat gain Q J/s	$(T_s - T_{av})$ ^oC	Useful heat gain Q J/s
m_1	8.938	35.881	12.598	56.162
m_2	8.077	45.242	10.319	82.001
m_3	6.966	40.951	8.903	75.078

The bar diagrams shown in figures 6 and 7 represents the plain duct configuration and the reflector duct configuration in terms of convective heat transfer coefficient and Nusselt number respectively. It is seen from fig. 7 that the Nusselt number shows a marginal improvement of 11% for reflector duct configuration at lower mass flow rate m_1. However at intermediate mass flow rate m_2, the increase in the Nusselt number is 40% and is highest at 44% for the highest mass flow rate m_3. A similar percentage rise is observed for the convective heat transfer coefficient for the two configurations as seen in fig. 6. As the mass flow rate increases the difference in Nusselt number between the reflector configuration and plain configuration increases. This can be attributed to the fact that the turbulence in reflector configuration becomes more vigorous due to three sides of duct contributing radiation heat to the absorber air.

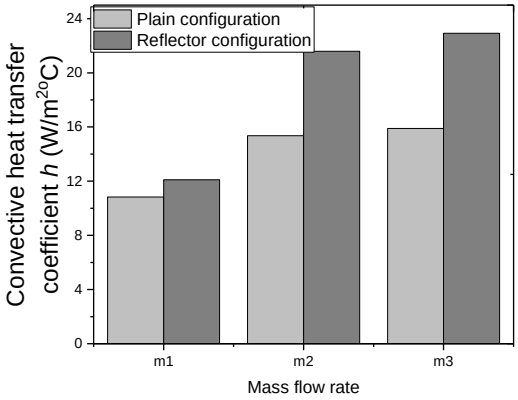

Figure 6. Convective heat transfer coefficient for the two configuration corresponding to the three mass flow rates.

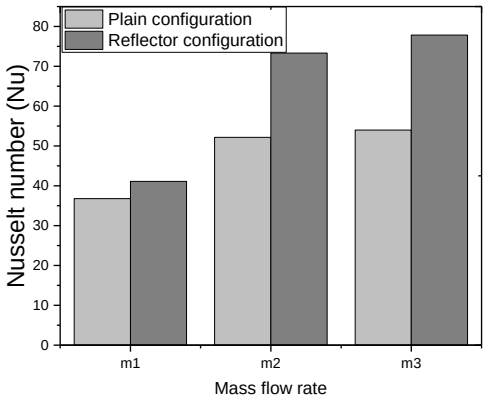

Figure 7. Nusselt number for the two configurations corresponding to the three mass flow rates

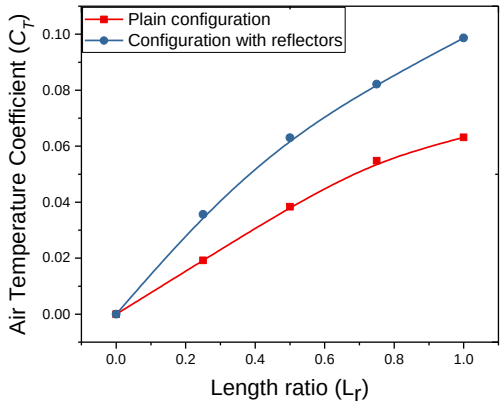

Figure 8. Temperature coefficient of absorber air along the flow path for lower mass flow rate m_1

Figures 8 to 10 show the variation of absorber air temperature coefficient (C_T) with the length ratio (L_r) corresponding to low, intermediate and high mass flow rates. The air temperature coefficient increases along the length of the absorber duct. At the entrance (L_r = 0), both the configurations have the same temperature (T_i). However as the fluid moves within the duct, the difference between the

temperature of the absorber air for reflector and plain configurations shows a diverging trend with significant rise in the temperature of air for the reflector configuration. This can be due to the reason that in the reflector configuration, the temperature of the fluid rises because of convective heat transfer taking place from both the side walls of the duct along with the top surface unlike the plain configuration.

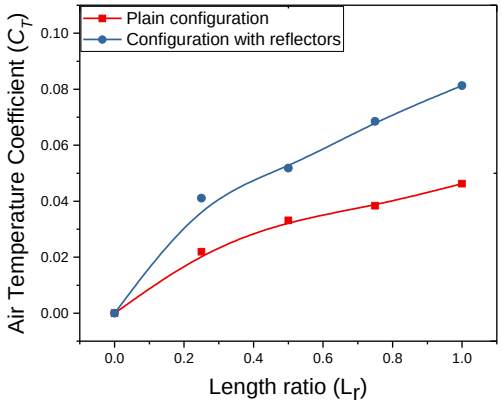

Figure 9. Temperature coefficient of absorber air along the flow path for intermediate mass flow rate m_2

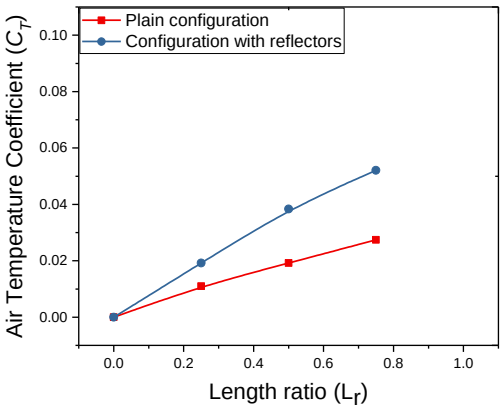

Figure 10. Temperature coefficient of absorber air along the flow path for higher mass flow rate m_3

Figure 11 shows absorber plate temperature coefficient across the duct for varying mass flow rates in terms of Reynolds number. It is seen from fig. 11 that the average temperature of absorber duct decreases with increase in mass flow rate. This can be attributed to the reason that the temperature is higher for slow moving fluid compared to that of fast moving fluid. Higher the Reynold's number better is the heat transfer as the high velocity fluid carries away the heat from the absorber plate. The absorber plate temperature is higher for reflector configuration as the duct receives radiation heat on three sides of the duct unlike that of plain duct configuration.

The absorber plate temperature distribution across the flow length is shown in fig. 12. It can be observed from this figure that the absorber plate temperature increases with the flow length to a high and then decreases marginally. Also it can be seen that the absorber plate temperature decreases with increase in mass flow rate. The peak point in the temperature profile can be attributed to the reason that the absorber air gets heated as it moves towards the exit and hence the absorber plate temperature does not get cooled as much as in the upstream region. However near to the downstream, the cooler layer of air from the mid height region replaces the hot air layer just below the absorber plate due to turbulence and exit boundary conditions. Hence we see a marginal drop in absorber plate temperature near the exit compared to the intermediate flow region.

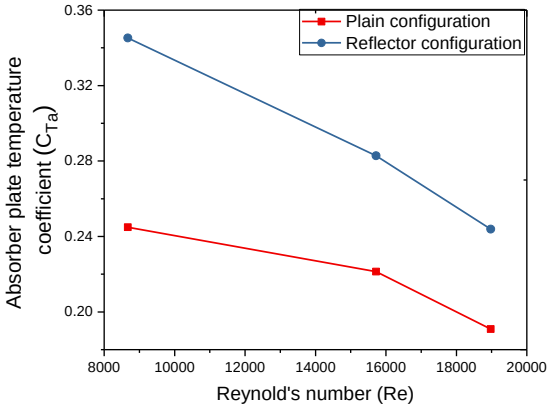

Figure 11. Plot of absorber plate temperature coefficient with respect to Reynolds's number.

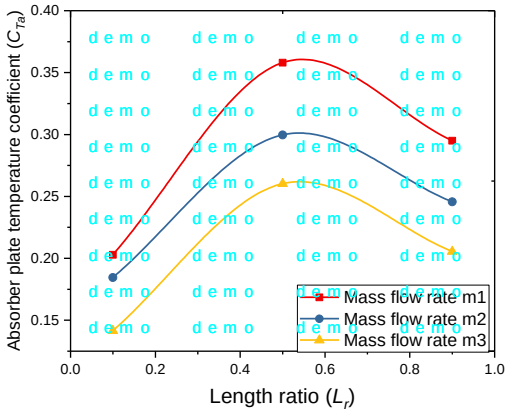

Figure 12. Plot of absorber plate temperature coefficient versus flow length ratio for the plain configuration

Fig. 13 shows a plot of the radiation heat flux with respect to time ratio. The heat flux due to radiation normal to the top surface of the air heater changes with time ratio. It can be observed from this graph that there exists a wide gap between the normal radiation heat flux and the reflected radiation heat flux. This is due to the 10 – 15% radiation loss that occurs in the reflector material.

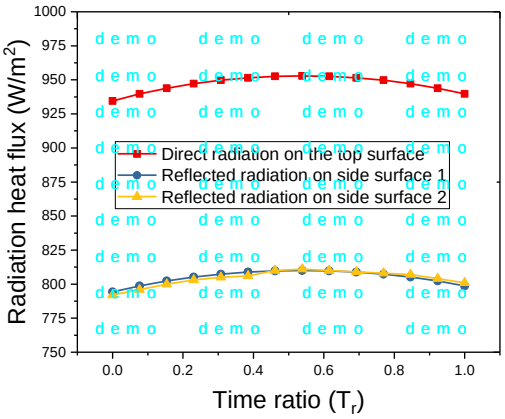

Figure 13. Radiation heat flux incident on the absorber duct with respect to time

CONCLUSIONS

Experimental study of square duct solar air heater with side reflectors is carried out and compared with that of a square duct solar air heater without reflectors, the following conclusions are drawn from the study:

a. Solar air heater with side reflectors shows a significant improvement in temperature of the absorber air compared to that of the configuration without reflectors.

b. It is observed that the net temperature rise across the duct decreases with increase in mass flow rate.

c. The configuration with reflectors shows a remarkable improvement in terms of thermal performance with the convective heat transfer coefficient and Nusselt Number showing a maximum of 44 % improvement over the plain configuration.

d. Higher the mass flow rate higher is the difference in Nusselt number between the reflector configuration and plain configuration as the turbulence in reflector configuration is more vigorous due to three sides of duct contributing radiation heat to the absorber air.

e. It is inferred that absorber plate temperature of the configuration with reflectors is greater than that of the plain configuration as three sides of the absorber duct are contributing towards the temperature rise as compared to the plain configuration.

f. The turbulent mixing of air in the absorber duct of reflector configuration is more pronounced than that of plain configuration as the three side heating changes the flow dynamics of the air inside the duct.

Nomenclature

T_i = Ambient temperature in ^oC,

T_o = Exit temperature of air after heating in ^oC,

T_{av} = Average air temperature inside the duct ^oC,

T_s = Average absorber duct temperature in ^oC,

V = velocity of air in m/s,

$\dot{m}$ = mass flow rate in kg/s,

ρ = Density of air in kg/m^3,

C_p = Specific heat of air in J/kg^oC,

ν = kinematic viscosity of air in m^2/s

Q = Rate of heat transfer in J/s

Re = Reynold's number,

Pr = Prandtl number,

Nu = Nusselt number,

A_s = Surface area of absorber plate in m^2,

T_r = Time ratio = *Time t/Total* time in min.

REFERENCES

[1] Abdul-Malik E.M., Saini JS, Solanki S.C., "Heat transfer and friction in solar air heater duct with V-shaped rib roughness on absorber plate", *International Journal of Heat and Mass Transfer,* Vol. 45 2002, pp. 3383–3396.

[2] Brij Bhushan., Ranjit Singh, "Nusselt number and friction factor correlations for solar air heater duct having artificially roughened absorber plate", *Journal of Solar Energy,* Vol. 85, 2011, pp. 1109–1118.

[3] Bhagoria J.L., Saini J.S., Solanki S.C., "Heat transfer coefficient and friction factor correlations for rectangular solar air heater duct having transverse wedge shaped rib roughness on the absorber plate", *Journal of Renewable Energy*, Vol. 25, 2002, pp. 341–369.

[4] Hans V.S., Saini R.P., Saini J.S., "Heat transfer and friction factor correlations for a solar air heater duct roughened artificially with multiple V-ribs", *Journal of Solar Energy*, Vol. 84, 2007, pp. 898–911.

[5] Kumar K., Prajapati D.R., Samir S., "Determination of effective efficiency of artificially roughened solar air heater duct using ribs", *Journal of Distribution General Alternate Energy*, Vol. 30, 2015, pp. 57–77.

[6] Layek A, Saini JS, Solanki S. C., "Second law optimization of solar air heater having chamfered rib groove roughness on absorber plate", *Journal of Renewable Energy,* Vol. 32, 2007, pp. 1967–1980.

[7] Mohamad A. A., (), "High-efficiency solar air heater", Journal of Solar Energy, Vol. 60, pp. 71–76.

[8] Muluwork K.B, "Investigations on fluid flow and heat transfer in roughened absorber solar heaters", PhD dissertation, IIT Roorkee. 2000.

[9] Rosenhow, W.M., Hartnett, J.P., Handbook of Heat Transfer. McGraw Hill, New York, 1973, pp. 7–122.

[10] Varun, R.P. Saini, S.K. Singal,"Investigation of thermal performance of solar air heater having

roughness elements as a combination of inclined and transverse ribs on the absorber plate", *Journal of Renewable Energy,* Vol. 33, 2008, pp. 1398–1405.

[11] Verma SK, Prasad BN, "Investigation for optimal thermohydraulic performance of artificially roughened solar air heaters", *Journal of Renewable Energy*, Vol. 20, 2000, pp. 19–36.